

Measuring the centroid gain of a Shack–Hartmann quad-cell wavefront sensor by using slope discrepancy

Marcos A. van Dam

W. M. Keck Observatory, 65-1120 Mamalahoa Highway, Kamuela, Hawaii 96743

Received October 8, 2004; revised manuscript received December 7, 2004; accepted February 7, 2005

Shack–Hartmann wavefront sensors (SH WFS) are used by many adaptive optics (AO) systems to measure the wavefront. In this WFS, the centroid of the spots is proportional to the wavefront slope. If the detectors consist of 2×2 quad cells, as is the case in most astronomical AO systems, then the centroid measurement is proportional to the centroid gain. This quantity varies with the strength of the atmospheric turbulence and the angular extent of the beacon. The benefits of knowing the centroid gain and current techniques to measure it are discussed. A new method is presented, which takes advantage of the fact that, in a SH-WFS-based AO system, there are usually more measurements than actuators. Centroids in the null space of the wavefront reconstructor, called slope discrepancy measurements, contain information about the centroid gain. Tests using the W. M. Keck Observatory AO system demonstrate the accuracy of the algorithm. © 2005 Optical Society of America
OCIS codes: 010.1080, 010.7350.

1. INTRODUCTION

Adaptive optics (AO) systems have been implemented at many astronomical observatories, with spectacular results.¹ A key component in an AO system is the wavefront sensor (WFS). Most WFSs measure wavefront derivatives, from which the wavefront can be reconstructed and compensated in real time. The most widely used WFS is the Shack–Hartmann (SH) WFS, which subdivides the pupil by using a lenslet array and focuses the light on each subaperture onto the focal plane.^{1,2} The displacement of the spots imaged at the focal plane of the detector is proportional to the wavefront slope.

If the displacement of the spot is measured by taking the centroid by using a large number of pixels, then the magnitude of the centroid estimate is independent of the spot size. The wavefront slope can also be estimated by using an array of only 2×2 pixels per subaperture, known as a quad cell. Quad cells produce centroid estimates that are, to a good approximation, linear with the displacement of a Gaussian spot for centroids with an absolute value of less than 0.5. The advantage of using quad cells lies in the speed of readout and computation and a reduction in noise, since fewer pixels are read. For these reasons, most astronomical AO systems employ quad cells: Among these are AO systems at the Lick, Palomar,³ Gemini North, and Keck observatories.⁴ The principal disadvantage of using quad cells lies in the fact that the centroid measurement is proportional to the centroid gain.⁵ The centroid gain is the relationship between the quad-cell centroid and the displacement of the spot (or, alternatively, the wavefront slope), a quantity that is inversely proportional to the spot size. Since the spot size is not known *a priori* and depends on the strength of the atmospheric turbulence and the angular extent of the beacon used by the WFS, the centroid gain is not known either. A technique is presented in this paper to track

variations in the centroid gain caused by changes in either the seeing or the extent of the beacon. It relies on the fact that there are components of the WFS measurements that are not affected by the AO system because the wavefront reconstructor is blind to them. These components yield a signal proportional to the centroid gain. A time-evolving estimate of the centroid gain is obtained by measuring the component of the centroids that the reconstructor cannot see.

In practice, the lack of knowledge of the centroid gain is mitigated by the fact that all existing AO systems operate in closed loop, so the spots are iteratively driven toward the center of the quad cells. Two problems associated with the uncertainty in the spot size remain; these issues are discussed in much greater detail in the work of Véran and Herriot.⁵

First, the gain of the feedback loop is proportional to the centroid gain. Knowledge of the loop gain is necessary to estimate and reduce the bandwidth and noise errors of the AO system,^{4,5} which are the two dominant error terms when the beacon is faint. An AO system with a SH WFS uses a wavefront reconstructor matrix to convert slope measurements into actuator voltages in the deformable mirror (DM). The reconstructor is typically computed via a singular-value decomposition or least-squares inversion of the influence matrix. The influence matrix is calculated by placing an unresolved calibration light source at the focus of the telescope, poking the actuators one by one, and measuring the centroids. However, the centroid gain will be different when the wavefront sensing is performed by using an object on the sky instead of the calibration source as the beacon. Assuming that the spots are all the same size, the influence matrix, and hence the reconstructor matrix and the overall loop gain, will be off by a constant gain factor.

Second, a change in the centroid gain introduces static

aberrations. To mitigate the effect of non-common-path aberrations, the shape that produces the best image on the science camera is placed on the DM during the calibration process. The centroids that are measured on the WFS are subsequently used as references.⁴ Alternatively, the image is sharpened in closed loop by modifying the reference centroids until the best image is attained.³ In either case, the magnitude of the reference centroids depends on the centroid gain. In closed-loop operation, the AO system attempts to null the difference between the measured centroids and the reference centroid. If the centroid gain changes, the calibrated reference centroids are wrong by a constant factor, and the AO system will drive the spots to the wrong position, thereby introducing a static aberration.

The remainder of the paper is organized as follows. Section 2 describes methods currently used to measure the centroid gain. This is followed by an introduction to the concept of slope discrepancy in Section 3 and how it can be used to measure the centroid gain in Section 4. Experimental results obtained at the Keck Observatory follow in Section 5, and conclusions are drawn in Section 6.

2. EXISTING METHODS FOR MEASURING THE CENTROID GAIN

In this section, we present and discuss existing methods that measure the centroid gain. In principle, it is also possible to infer the centroid gain by making seeing measurements and using knowledge of the angular extent of the beacon.

As mentioned in Section 1, an aberration is placed on the DM during calibration to compensate for non-common-path aberrations. Véran and Herriot proposed monitoring the shape of the DM as a way to measure the spot size on Altair, the AO system at Gemini North.^{5,6} If the centroid gain decreases but the reference centroids remain unchanged, the AO system will introduce a larger amount of this aberration than is needed to compensate for the non-common-path aberrations. Monitoring the average shape of the DM over time scales of a few seconds during nighttime operations and correlating it with the calibration shape yields a signal directly related to the centroid gain. Most of the power of the non-common-path aberrations is contained in the first few Zernike modes. Unfortunately, most of the power of the telescope primary mirror's aberrations also tends to be low order, and fluctuations in the shape of the primary mirror corrupt the centroid gain measurement.⁷

The following technique was also implemented on Altair.⁷ The tip-tilt mirror is dithered with an amplitude of 5 milliarcsec and an oscillation frequency equal to a quarter of the frame rate of the AO system. A lock-in detection algorithm is used to extract an estimate of the tip-tilt dithering amplitude in centroid units, and hence of the centroid gain, with a bandwidth of about 10 s. Although this method estimates the centroid gain successfully, it introduces a wavefront error of about 50 nm rms. Because the tip-tilt mirror has significant oscillations at high frequencies, the method was modified to dither the DM instead by adding focus and measuring the focus on the WFS.

A low-bandwidth wavefront sensor (LBWFS) has been implemented at the Keck Observatory to support the laser-guide-star AO program.⁸ With some modifications, it could also be used in natural guide star mode. There is a beam splitter located before the WFS that directs a small fraction of the light to the LBWFS. The LBWFS has the same number of subapertures as the WFS but a much larger number of pixels (16×16) per subaperture and much longer exposure times. The LBWFS detects slowly varying residual aberrations, and its centroid measurements can be used to change the reference centroids. By inspecting how the reference centroids change, one can also deduce the spot size on the WFS. For example, a doubling of the spot size will result in the reference centroids having half the magnitude relative to their calibration value.

The advantage of using a LBWFS is that the centroid gain can be estimated on a subaperture-by-subaperture basis. The disadvantages of this technique are the additional hardware and software required and the need to divert light away from the WFS.

3. SLOPE DISCREPANCY

In this section, a short tutorial on the concept of slope discrepancy is presented. The reader is referred to an excellent paper by Tyler for a more in-depth study of the topic.⁹

For the SH WFS, the relationship between the measured slope, $\mathbf{s}=(s_x, s_y)^T$, and the wavefront, \mathbf{w} , is

$$\mathbf{s} = \nabla \mathbf{w}, \quad (1)$$

where $\nabla \mathbf{w}=(w_x \hat{\mathbf{x}}, w_y \hat{\mathbf{y}})$ is the gradient operator acting on \mathbf{w} . Equation (1) can be written as a matrix multiplication:

$$\mathbf{s} = H \mathbf{w}. \quad (2)$$

The influence matrix, H , can be obtained from geometric considerations or from poking the actuators of the DM one at a time and recording the centroids. The least-squares estimate of \mathbf{w} , $\hat{\mathbf{w}}$, is given by

$$\hat{\mathbf{w}} = (H^T H)^+ H^T \mathbf{s}, \quad (3)$$

where the symbol $+$ denotes the pseudoinverse and $R=(H^T H)^+ H^T$ is the least-squares reconstructor. The pseudoinverse is required because the WFS is blind to the piston mode and, in the case of the Fried geometry,¹⁰ where the actuators are optically conjugate to the corners of the lenslets, to the waffle mode. The waffle mode is when adjacent actuators are alternatively up or down in a checkerboard pattern.

The column space of a matrix is the subspace spanned by its columns. The component of the slopes in the column space of R is⁹

$$\mathbf{s}_{\parallel} = H \hat{\mathbf{w}}, \quad (4)$$

where the subscript \parallel represents the column space of the reconstructor. The null space of R consists of all vectors \mathbf{s} such that $R \mathbf{s} = 0$.¹¹ Here, we use the symbol \perp to denote the null space of R . The slope discrepancy, \mathbf{s}_{\perp} , is the difference between the measured slopes and the slopes obtained by differentiating the reconstructed wavefront:

$$\mathbf{s}_\perp = \mathbf{s} - \mathbf{s}_\parallel = [I - H(H^T H)^+ H^T] \mathbf{s}. \quad (5)$$

Geometrically, the slope discrepancy can be interpreted as a curl in the slope vector field.⁹

In the remainder of the paper, without loss of generality we consider the case of the Keck AO system: a SH WFS with 240 subapertures in the Fried geometry, making 480 measurements to drive 349 actuators. In general, reconstructors that perform better in the presence of noise than the least-squares reconstructor are employed so Eq. (5) cannot be used. At the Keck Observatory, R is a 349×480 matrix created by using a regularized least-squares inversion of H that takes into account the statistics of the turbulence and of the noise.^{4,12} Depending on the angle of the telescope pupil on the WFS, about 50 of the actuators are slaved, leaving about $480 - (349 - 50) = 181$ linearly independent rows.

R can be written as a singular-value decomposition:

$$R = USV^T, \quad (6)$$

where U is a 349×349 matrix, S is a 349×480 diagonal matrix with the 349 singular values as its diagonal entries, and V is a 480×480 matrix. The columns of V , corresponding to the (approximately 181) zero-valued singular values of S , constitute an orthonormal basis, Z , for the null space of R . We rewrite the slope discrepancy for the general case of an arbitrary reconstructor as

$$\mathbf{s}_\perp = ZZ^T \mathbf{s}. \quad (7)$$

4. MEASURING THE CENTROID GAIN BY USING SLOPE DISCREPANCY

In this section, the process for estimating the centroid gain by using slope discrepancy is described. Let us define the centroid measurement made by using an unresolved source, \mathbf{s} , to be given by the difference between the raw centroids on the same source, \mathbf{r} , and the reference centroids, \mathbf{c} :

$$\mathbf{s} = \mathbf{r} - \mathbf{c}. \quad (8)$$

The slope discrepancy component in the reference centroids on the calibration source, \mathbf{c}_\perp , is $\mathbf{c}_\perp = ZZ^T \mathbf{c}$, with a similar definition for \mathbf{r}_\perp .

The reference centroids are composed of aberrations introduced by the lenslet array, the imaging leg, and the beam splitter that splits the light to the two legs. Lenslet arrays are not perfect: Even in the absence of any external aberration, the spots on the CCD are not centered directly below the center of each lenslet but have random x and y displacements, leading to x and y centroids. A large fraction of the power of these centroids (in this case, about $181/480 = 38\%$) lies in the null space of the reconstructor matrix.

The centroid measurement made with a star as the beacon, \mathbf{s}^* , is the difference between the raw centroids on the star, \mathbf{r}^* , and the reference centroids for the star, \mathbf{c}^* :

$$\mathbf{s}^* = \mathbf{r}^* - \mathbf{c}^*. \quad (9)$$

Let us define the relative centroid gain, β , to be the centroid gain on the star divided by the centroid gain on the

calibration source, where β lies between 0 and 1. Then the raw centroid measured on the star is $\mathbf{r}^* = \beta \mathbf{r}$. To compensate for the difference between \mathbf{r} and \mathbf{r}^* , one should scale the reference centroids by a factor, α , as close to β as possible. Equation (9) can be written as

$$\mathbf{s}^* = \beta \mathbf{r} - \alpha \mathbf{c}, \quad (10)$$

where $\mathbf{c}^* = \alpha \mathbf{c}$. The value of \mathbf{s}^* is equal to \mathbf{s} only if $\beta = \alpha$. The method presented in this paper estimates the value of $\beta - \alpha$.

It follows that

$$\mathbf{s}_\perp^* = \beta \mathbf{r}_\perp - \alpha \mathbf{c}_\perp. \quad (11)$$

Since neither turbulence nor measurement noise leads to an overall slope discrepancy component,

$$E[\mathbf{r}_\perp] = \mathbf{c}_\perp, \quad (12)$$

where $E[\cdot]$ is the expected value operator. Let us define a slope discrepancy metric, g , consisting of the least-squares linear fit of \mathbf{s}_\perp^* to \mathbf{c}_\perp :

$$g = \frac{\mathbf{s}_\perp^{*T} \mathbf{c}_\perp}{\mathbf{c}_\perp^T \mathbf{c}_\perp}. \quad (13)$$

Using Eqs. (11) and (12),

$$\begin{aligned} E[g] &= \frac{E[(\beta \mathbf{r}_\perp - \alpha \mathbf{c}_\perp)]^T \mathbf{c}_\perp}{\mathbf{c}_\perp^T \mathbf{c}_\perp} \\ &= \frac{(\beta E[\mathbf{r}_\perp] - \alpha \mathbf{c}_\perp)^T \mathbf{c}_\perp}{\mathbf{c}_\perp^T \mathbf{c}_\perp} \\ &= \frac{(\beta - \alpha) \mathbf{c}_\perp^T \mathbf{c}_\perp}{\mathbf{c}_\perp^T \mathbf{c}_\perp} = \beta - \alpha. \end{aligned} \quad (14)$$

Equation (14) is the key result of the paper: The expected value of the slope discrepancy metric is equal to the difference between the true relative scaling of the centroids due to the changing spot size and the scaling of the reference centroids to compensate for this change. To calculate the metric, successive measurements of the centroids, \mathbf{s}^* , are taken on the sky and averaged. The slope discrepancy component of the average is then least-squares fitted to the slope discrepancy component of the reference centroids, according to Eq. (13). If the reference centroid scaling is correct, i.e., if $\beta = \alpha$, then $g = 0$.

The method presented here relies on the fact that some of the power in the reference centroids is contained in the null space of the reconstructor. If this is not the case, e.g., if the lenslet array is of extremely high quality, slope discrepancy could be induced by rotating the lenslet array through a very small angle (a fraction of a degree) with respect to the CCD. Almost all the power thus induced in the centroids lies in the null space of the reconstructor. The degradation in the performance of the AO system resulting from introducing such a small rotation is negligible. There are two reasons why an aberration smaller than those for other methods is needed. First, the atmosphere produces no power in the null space of the reconstructor, so the measurements are not corrupted. Second, every measurement gives an estimate of the change in the

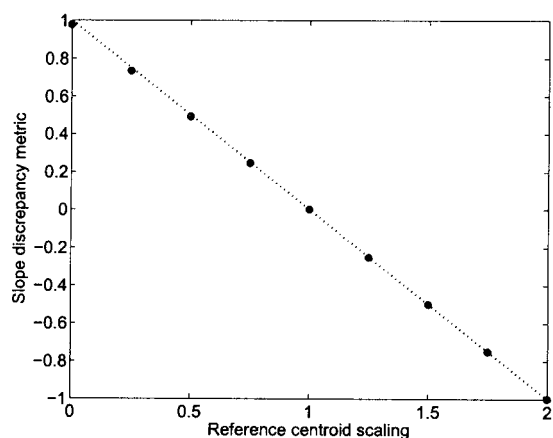


Fig. 1. Slope discrepancy metric, g , measured with the calibration light source as a function of reference centroid scaling, α .

response of the WFS, compared with dithering methods, where the measured signal needs to be correlated with the introduced signal. Furthermore, rotating the lenslet merely adds an aberration to which the reconstructor is blind.

5. EXPERIMENTAL RESULTS

A. Results with the Calibration Light Source

To verify the validity of the slope discrepancy approach under controlled conditions, it was implemented by using the calibration light source with no external turbulence. First, the DM was flattened by using an interferometer. Centroids were measured on the WFS in open loop and were defined to be the reference centroids. Then the tip-tilt and DM loops were closed, and a set of 1000 consecutive frames of centroid data was captured and averaged. This process was repeated with the reference centroids scaled by factors varying from zero to 2. The metric of Eq. (13) was calculated, and its average is displayed in Fig. 1, along with the results expected from theory. It can be seen that the slope of the curve is -1 and that the metric takes a value of 0 when the reference centroids are scaled correctly, as expected from Eq. (14).

B. Results on the Sky

The experiment of Subsection 5.A was then repeated on the sky and compared with two other independent methods for measuring the spot size on the two Keck telescopes.

1. Comparison with Image Displacement

The slope discrepancy metric as a function of reference centroid scaling on Keck II is displayed in Fig. 2. The least-squares fit has a slope of -1.04 and an x intercept of 0.76, indicating that the centroid gain is 0.76. A better estimate of the centroid gain can be obtained by simply averaging the sum of the slope discrepancy metric and the reference centroid scaling. This is equivalent to forcing the gradient to be equal to -1 and gives a centroid gain of 0.74.

To validate these results, another method was used to compute the centroid gain. Here, the loops are closed on the calibration source, and an image is taken on the sci-

ence camera. Then all the x or y reference centroids are offset by small constant amounts, ranging between -0.2 and 0.2 , and the displacements of the light source in the science image are measured. This procedure is then repeated by using a guide star on the sky. Since the displacement of the image is inversely proportional to the centroid gain, the ratio of the centroid gain with the calibration light source to the centroid gain on the sky can be calculated. This technique requires dedicated telescope time and is not suitable for use during a science observation. However, it is very accurate, and for this reason it is used for comparison with the slope discrepancy method.

Figure 3 plots the results with a star and with the calibration light source. The ratio of the gradient of these two curves is 0.82 for x (plotted) and 0.79 for y . The data taken for calculating the centroid gain by using these two methods were interleaved to eliminate the possibility of the seeing changing from one test to the next.

2. Comparison with Chopping

The slope discrepancy metric as a function of reference centroid scaling on Keck I on a different night is displayed in Fig. 4. The least-squares fit has a slope of -1.01 and an x intercept of 0.71, indicating that the centroid gain is 0.71.

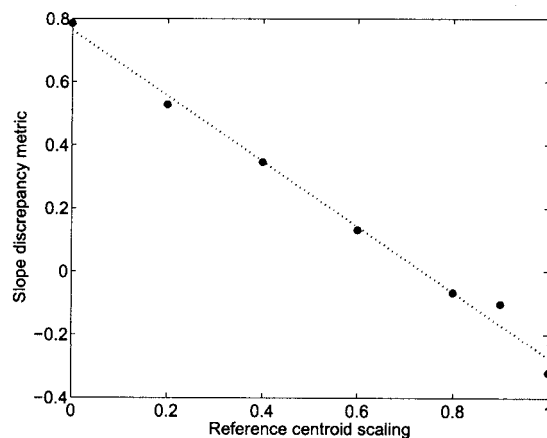


Fig. 2. Slope discrepancy metric, g , measured with a star as a function of reference centroid scaling, α , on Keck II.

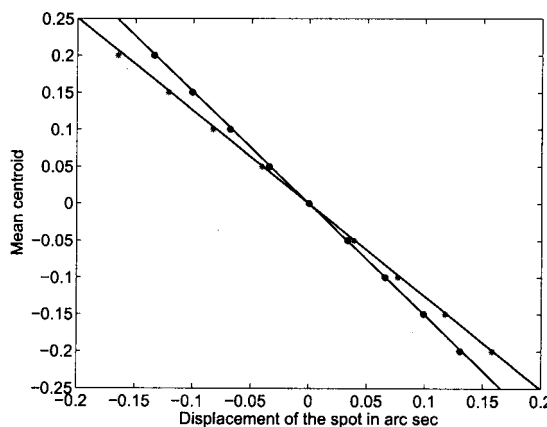


Fig. 3. Plot of the mean x -centroid value as a function of displacement of the star (asterisks) and calibration light source (circles).

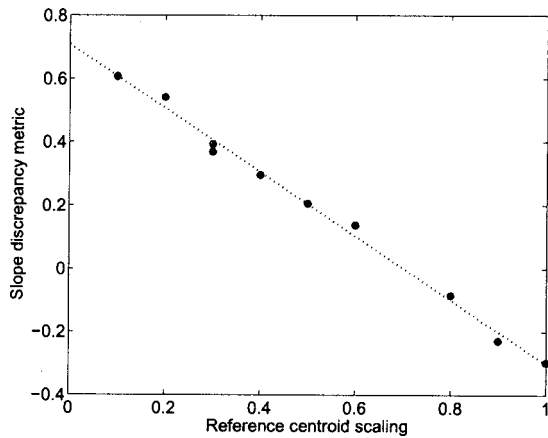


Fig. 4. Slope discrepancy metric, g , measured with a star as a function of reference centroid scaling, α , on Keck I.

A few minutes later, the centroid gain was measured in an independent way by chopping the tip-tilt mirror. The procedure is as follows. Both the tip-tilt and DM loops are closed. Then the reference centroids are offset by using a square wave with a frequency of 4 Hz and a magnitude that corresponds to a peak displacement of the mirror of 0.1 arcsec when the calibration source is used. The actual position of the mirror is monitored by using a strain gauge; this is equivalent to measuring the displacement of the spot. On the sky, the amplitude of the chop was determined to be 0.147 ± 0.007 arcsec, which implies that the centroid gain is $0.1/0.147 = 0.68 \pm 0.03$. Since the atmosphere also causes the tip-tilt mirror to be displaced, this method is not as reliable as that of Subsection 5.B.1.

C. Discussion

Results on the sky show that the slope discrepancy method produces accurate estimates of the centroid gain. Since the measurement is made by averaging over a large number of centroid vectors, the noise can be kept low, even when the guide star is very faint.

There is a slight inconsistency in the results with the image displacement method, and future work will concentrate on gathering more data and improving the reliability of the slope discrepancy estimates. The discrepancy is likely to consist of systematic errors due to partially illuminated subapertures, which have larger spots and are not as well controlled as fully illuminated subapertures. This adds some uncertainty to the measurements, especially in low-order AO systems, where a large proportion of the subapertures are only partially illuminated.

The accuracy of the slope discrepancy method should not be affected by the presence of turbulence. Atmospheric turbulence lies mostly in the column space of the reconstructor, since the job of the reconstructor is to reject turbulence, and any component in the null space is averaged over time. A possible source of systematic error could be high-spatial-frequency wavefront aberrations aliased onto lower-frequency aberrations. These aberrations could stem from either atmospheric turbulence¹³ or discontinuities in a segmented primary mirror.¹⁴ However, the inner product of these centroids with the slope discrepancy in the reference centroids is likely to be small.

Another possible source of error in the slope discrepancy metric is due to centroid errors that do not stem from optical effects. An example of this is the uncompensated flat field of the CCD.

6. CONCLUSION

It is very important to be able to estimate the centroid gain when using a SH WFS with quad cells. Several techniques have been proposed to measure the centroid gain, but they all require active modifications to the AO system that result in an increase in wavefront error. In this paper, a new technique is proposed that takes advantage of the fact that the AO system does not respond to centroids in the null space of the reconstructor. The linear fit of the centroids in the null space to the reference centroids in the null space gives a metric that is directly related to the centroid gain. Sky tests using the Keck Observatory adaptive optics systems have demonstrated the potential of this method.

ACKNOWLEDGMENTS

The author is grateful to David Le Mignant, Antonin Bouchez, and Erik Johansson for their assistance in collecting telescope data. This work was performed under the auspices of the U.S. Department of Energy by the University of California, Lawrence Livermore National Laboratory, under contract W-7405-Eng-48. The work has been supported by the National Science Foundation Science and Technology Center for Adaptive Optics, managed by the University of California at Santa Cruz under cooperative agreement AST-9876783. The data presented herein were obtained at the W. M. Keck Observatory, which is operated as a scientific partnership among the California Institute of Technology, the University of California, and the National Aeronautics and Space Administration. The observatory was made possible by the generous financial support of the W. M. Keck Foundation. The author recognizes and acknowledges the significant cultural role and reverence that the summit of Mauna Kea has always had within the Hawaiian community. We are most fortunate to have the opportunity to conduct observations from this mountain.

M. A. van Dam may be reached by e-mail at mvandam@keck.hawaii.edu.

REFERENCES

1. J. W. Hardy, *Adaptive Optics for Astronomical Telescopes* (Oxford U. Press, 1998).
2. M. C. Roggemann and B. Welsh, *Imaging through Turbulence* (CRC Press, 1996).
3. M. Troy, R. G. Dekany, G. Brack, B. R. Oppenheimer, E. E. Bloemhof, T. Trinh, F. G. Dekens, F. Shi, T. L. Hayward, and B. Brandl, "Palomar adaptive optics project: status and performance," in *Adaptive Optical Systems Technology*, P. L. Wizinowich, ed., Proc. SPIE **4007**, 31–40 (2000).
4. M. A. van Dam, D. Le Mignant, and B. A. Macintosh, "Performance of the Keck Observatory adaptive optics system," *Appl. Opt.* **43**, 5458–5467 (2004).
5. J. P. Véran and G. Herriot, "Centroid gain compensation in

- Shack–Hartmann adaptive optics systems with natural or laser guide star,” *J. Opt. Soc. Am. A* **17**, 1430–1439 (2000).
6. J. P. Véran and G. Herriot, “Centroid gain compensation in a Shack–Hartmann adaptive optics system: implementation issues,” in *Adaptive Optical Systems Technology*, P. L. Wizinowich, ed., Proc. SPIE **4007**, 642–648 (2000).
 7. L. K. Saddlemyer, G. Herriot, J.-P. Véran, M. Smith, and J. Dunn, “Innovations within the Altair real-time wave-front reconstructor,” in *Astronomical Adaptive Optics Systems and Applications*, D. Bonaccini, B. L. Ellerbroek, and R. Ragazzoni, eds., Proc. SPIE **5490**, 1384–1392 (2004).
 8. A. H. Bouchez, D. Le Mignant, M. A. van Dam, J. Chin, S. Hartman, E. Johansson, R. Lafon, P. Stomski, D. Summers, and P. L. Wizinowich, “Keck laser guide star adaptive optics: science verification results,” in *Advancements in Adaptive Optics*, D. Bonaccini, B. L. Ellerbroek, and R. Ragazzoni, eds., Proc. SPIE **5490**, 321–330 (2004).
 9. G. A. Tyler, “Reconstruction and assessment of the least-squares and slope discrepancy components of the phase,” *J. Opt. Soc. Am. A* **17**, 1828–1839 (2000).
 10. R. H. Hudgin, “Wave-front reconstruction for compensated imaging,” *J. Opt. Soc. Am.* **67**, 375–378 (1977).
 11. G. Strang, *Linear Algebra and Its Applications*, 3rd ed. (Harcourt Brace, 1988).
 12. M. A. van Dam, D. Le Mignant, and B. A. Macintosh, “Characterization of adaptive optics at Keck Observatory: part II,” in *Advancements in Adaptive Optics*, D. Bonaccini, B. L. Ellerbroek, and R. Ragazzoni, eds., Proc. SPIE **5490**, 174–183 (2004).
 13. F. J. Rigaut, J. Veran, and O. Lai, “Analytical model for Shack–Hartmann-based adaptive optics systems,” in *Adaptive Optical System Technologies*, D. Bonaccini and R. K. Tyson, eds., Proc. SPIE **3353**, 1038–1048 (1998).
 14. G. Chanan, C. Ohara, and M. Troy, “Phasing the mirror segments of the Keck telescopes II: the narrow-band phasing algorithm,” *Appl. Opt.* **39**, 4706–4714 (2000).